JOURNAL OF AGRICULTURAL AND FOOD CHEMISTRY

Article

pubs.acs.org/JAFC

Toxicological Mechanisms of Nanosized Titanium Dioxide-Induced Spleen Injury in Mice after Repeated Peroral Application

Xuezi Sang,[†,∥] Bing Li,[†,∥] Yuguan Ze,[†,∥] Jie Hong,[†,∥] Xiao Ze,[†] Suxin Gui,[†] Qingqing Sun,[†] Huiting Liu,[†] Xiaoyang Zhao,[†] Lei Sheng,[†] Dong Liu,[†] Xiaohong Yu,[†] Ling Wang,[†] and Fashui Hong*[,†,‡,§]

[†]Medical College of Soochow University, Suzhou 215123, China

[‡]Jiangsu Province Key Laboratory of Stem Cell Research, Soochow University, 708 Renmin Road, Suzhou 215007, China

[§]Cultivation base of State Key Laboratory of Stem Cell and Biomaterials built together by Ministry of Science and Technology and Jiangsu Province, Suzhou 215007, China

ABSTRACT: Due to an increase in surface area per particle weight, nanosized titanium dioxide (nano-TiO_2) has greatly increased its function as a catalyst and is used for whitening and brightening foods. However, concerns over the safety of nano-TiO_2 have been raised. The purpose of this study was to determine whether the protein kinase MAPKs/PI3-K/Akt signaling pathways and transcription factors are activated prior to or concurrent with COX-2 up-regulation in mouse spleen following exposure to 10 mg/kg BW of pure anatase nano-TiO_2 by the intragastric route for 15−90 days. The study clearly showed that nano-TiO_2 was deposited in the spleen and resulted in reactive oxygen species production, time-dependent splenic inflammation, and necrosis, coupled with a 12.64−64.06% increase in COX-2 and prostaglandin E2 expression, respectively. Furthermore, nano-TiO_2 elevated the expressions of ERK, AP-1, CRE, Akt, JNK2, MAPKs, PI3-K, c-Jun, and c-Fos in the spleen by 1.08−6-fold with increased exposure duration, respectively. These findings suggested that nano-TiO_2-induced COX-2 expression may be mediated predominantly through the induction of AP-1 and CRE and that AP-1/CRE induction occurred via the MAPKs/PI3-K/Akt signaling pathways in the spleen. Therefore, the findings suggest the need for caution when using nanomaterials as food additives.

KEYWORDS: *nanosized titanium dioxide, spleen damage, cyclooxygenase-2, cyclic adenosine monophosphate-response element, MAPKs/PI3-K/Akt signaling pathways*

INTRODUCTION

The quantity of titanium dioxide (non-nano-TiO_2) should not exceed 1% by weight of food according to federal regulations of the U.S. government and "quantum satis" in the European Union (EU). In 1999 the U.S. Food and Drug Administration (FDA) allowed the use of nanoparticles in sunscreens. In addition, the food industry is beginning to introduce nano-TiO_2 and other nanomaterials as food additives, as food packaging components, and in crop production or as dietary supplements due to its whitening and brightening properties,[1−4] and in the degradation and treatment of winery wastewaters and pesticides due its photocatalytic properties.[5,6] The potential toxic effects of nano-TiO_2 and its effect on human health are gaining increasing attention, as nano-TiO_2 possesses novel properties that are different from those of microsized TiO_2 material. Recent papers have also suggested that nano-TiO_2 plays an important role in triggering biological responses in the spleen of mice. For example, nano-TiO_2 was demonstrated to induce pathological changes such as increased neutrophil numbers,[7] lymph node cell proliferation, reduction,[8] and apoptosis in mouse spleen[9] and exerted its toxicity through oxidative stress.[6] These studies also showed that exposure to nano-TiO_2 activated the expression of p38, nuclear factor-κB (NF-κB), nuclear factor-E2-related factor-2 (Nrf-2), c-Jun N-terminal kinase (JNK), heme oxygenase-1 (HO-1), tumor necrosis factor-α (TNF-α), macrophage migration inhibitory factor (MIF), interleukin-2 (IL-2), IL-4, IL-6, IL-8, IL-10, IL-18, IL-1β, C-reactive protein (CRP), transforming growth factor-β (TGF-β), interferon-γ (IF-γ), Bax, and CYP1A1 and decreased the levels of IκB, Bcl-2, and heat shock protein 70 expression, thus resulting in impairment of immune function in the spleen.[8−10] These studies focused on the dose-dependent toxicities of nano-TiO_2 on spleen damage. However, the time-dependent toxicities of nano-TiO_2 applied perorally on spleen damage have not been investigated, and the exact mechanisms underlying the adverse effects of nano-TiO_2 on spleen following exposure remain unclear.

It is known that cyclooxygenase (COX)-2 is an essential enzyme involved in inflammatory processes and other pathogenetic processes.[11] COX-1 and COX-2 are the two isoforms of COX. COX-1 is constitutively expressed in many cell types, and COX-2 is induced when inflammation occurs.[11] It has been suggested that COX-2 expression and its activation are induced in mouse lung following acute lung injury.[12] Numerous mediators are associated with organ inflammation. For example, prostaglandins (PGs) are induced by COX-2, which may play a key role in the inflammatory process in organs.[13] PG synthesis is initiated by the release of arachidonic acid from the plasma membrane caused by phospholipase A2 (PLA2) and then converted to PGH2 by COX-2.[14,15] PGs are small lipid molecules

Received: August 20, 2012
Revised: April 13, 2013
Accepted: April 26, 2013
Published: April 26, 2013

Table 1. Real-Time PCR Primer Pairs Used in the Gene Expression Analysis

gene name	description	primer sequence	primer size (bp)
refer-actin	m actin F	5′-GAGACCTTCAACACCCCAGC-3′	
	m actin R	5′-ATGTCACGCACGATTTCCC-3′	263
COX-2	mCOX-2 F	5′-GTGGAAAAACCTCGTCCAGA-3′	
	mCOX-2 R	5′-TGATGGTGGCTGTTTTGGTA-3′	256
PGE2	mPEG2 F	5′-CCAGGACGGAGGAGATGAAGTG-3′	
	mPEG2 R	5′-CCAGGCrGGATGAGTGAGTGTT-3′	307
CRE	mCRE F	5′-TACGGATGGGGTACAGGGC-3′	
	mCRE R	5′-CAATGGTGCTCGTGGGTG-3′	197
AP-1	mAP-1 F	5′-GTTCCTTCCATATCTTCTGCTGGG-3′	
	mAP-1 R	5′-GAGGTGCGTGCACTTGTGAATCAT-3′	370
Akt	mAkt F	5′-GAGCATCATCCCTGGGTTAC-3′	
	mAkt R	5′-CTCCTTCACAATGGCTACG-3′	400
PI3-K	mPI3-K F	5′-TTCCAGCCTGGGTAACAAAG-3′	
	mPI3-K R	5′-CGTCAG AACAAGACCCTGTG-3′	890
MAPKs	mMAPKs F	5′-CGACAGTGATCACTAGTTGT-3′	
	mMAPKs R	5′-GCAGAATTTAGGCCGTCATC-3′	235
JNK	mJNK F	5′-TCTCCAGCACCCATACATCAA-3′	
	mJNK R	5′-TCCTCCAAATCCATTACCTCC-3′	142
ERK	mERK F	5′-ACACCTCCCCCAAGAATACAG-3′	
	mERK R	5′-GCTCATCCTCAACACCACAG-3′	477
c-Jun	mc-Jun F	5′-TGGGATTACACGTGTGAACCAACC-3′	
	mc-Jun R	5′-TGTGACACAGGCAGACTGTGGATC-3′	123
c-Eos	mc-Fos F	5′-AACGGTCACCGCAATCAC-3′	
	mc-Fos R	5′-GGCATGTCATAAGGGTCAAC-3′	80

involved in the modulation of numerous processes including the regulation of immune function, kidney function, platelet aggregation, and neurotransmitter release.[16,17] In COX-2 gene expression, promoter elements for NF-κB, NF-IL6, and activator protein 1 (AP-1)/cyclic adenosine monophosphate (cAMP)-response element (CRE) have been shown to be important for regulating transcription.[18−25] However, the relative contribution of the various promoter elements to COX-2 transcription in macrophages is not completely understood. Tumor promoters including 12-*O*-tetradecanoylphorbol-13-acetate (TPA), epidermal growth factor (EGF), and TNF-α have been demonstrated to induce AP-1 activity and neoplastic transformation by activating MAPK including extracellular signal-regulated kinase (ERK), JNK, or p38 kinase in the mouse epidermal cell.[26] Many inflammation-related factors that induce COX-2 gene expression can also activate MAPKs and PI3-K/serine/threonine kinase protein kinase B (Akt).[27−30] MAPKs are serine/threonine protein kinases that govern various cellular processes, including cell growth, proliferation, differentiation, and apoptosis. The effect of MAPK on gene expression depends on the cellular and stimulatory context. Here, we hypothesized that following exposure to nano-TiO_2 the MAPKs/PI3-K/Akt signaling pathways and transcription factors may be activated prior to or concurrent with COX-2 gene up-regulation in mice with spleen injury.

Although the use of nano-TiO_2 is permitted in the food industry, the safety of nano-TiO_2 following increased exposure duration requires further evaluation. Therefore, in this study, we aimed to investigate dynamic spleen damage due to increased exposure duration to nano-TiO_2, the effects of nano-TiO_2 on prostaglandin E2 (PGE2) and COX-2 expression, and

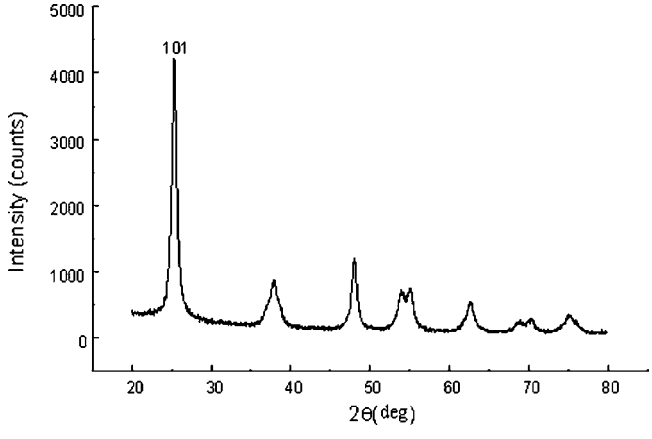

Figure 1. (101) X-ray diffraction peak of anatase TiO_2 NPs. The average grain size was about 5 nm by calculation of Scherrer's equation.

dx.doi.org/10.1021/jf3035989 | J. Agric. Food Chem. 2013, 61, 5590−5599

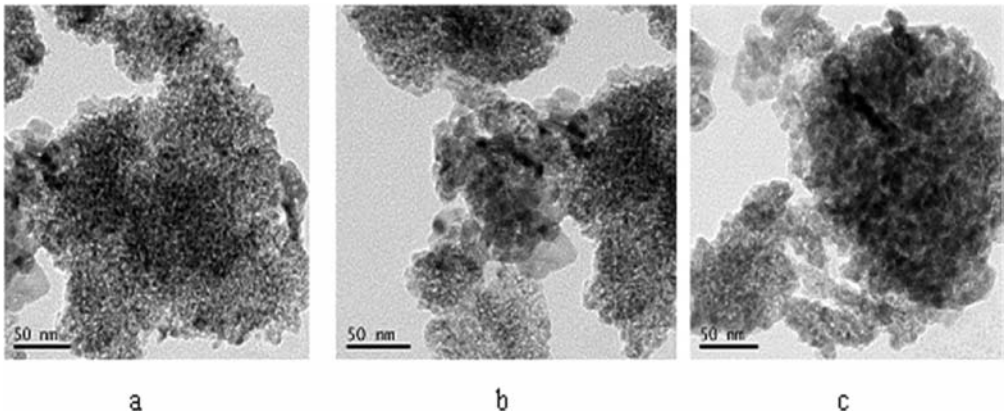

Figure 2. Transmission electron microscope images of anatase TiO_2 NPs particles: (a) TiO_2 NPs powder; (b) TiO_2 NPs suspended in HPMC solvent after incubation for 12 h; (c) TiO_2 NPs suspended in HPMC solvent after incubation for 24 h. TEM images showed that the sizes of the TiO_2 NPs in powder or suspended in HPMC solvent for 12 or 24 h were distributed from 5 to 6 nm, respectively.

nano-TiO_2-induced expression of the COX-2 gene to determine whether this expression is regulated at the level of MAPKs and transcription factors in mouse spleen following different exposure periods. Furthermore, the role of AP-1 and CRE in nano-TiO_2-mediated MAPK/PI3-K/Akt activation was examined in damaged spleen following increased exposure duration. Our findings suggested that with increased exposure duration, nano-TiO_2 caused significant splenomegaly, lymphocyte proliferation, macrophage infiltration, fatty degeneration, and cell necrosis in the spleen, which was closely related to increased COX-2, PGE2, AP-1, CRE, Akt, PI3-K, MAPKs, JNK, ERK, c-Jun, and c-Fos expression.

MATERIALS AND METHODS

Chemicals. Anatase TiO_2 nanoparticles were prepared via controlled hydrolysis of titanium tetrabutoxide. The details of nano-TiO_2 synthesis were previously described.[31,32] Briefly, colloidal titanium dioxide was prepared via the controlled hydrolysis of titanium tetrabutoxide. In a typical experiment, 1 mL of $Ti(OC_4H_9)_4$ was dissolved in 20 mL of anhydrous isopropanol and was added dropwise to 50 mL of double-distilled water, which was adjusted to pH 1.5 with nitric acid under vigorous stirring at room temperature. The temperature of the solution was then raised to 60 °C and maintained for 6 h to promote better crystallization of TiO_2 nanoparticles. Using a rotary evaporator, the resulting translucent colloidal suspension was evaporated to yield a nanocrystalline powder. The obtained powder was washed three times with isopropanol and then dried at 50 °C until evaporation of the solvent was complete. Hydroxypropylmethylcellulose (HPMC) 0.5% w/v was used as a suspending agent. TiO_2 powder was dispersed onto the surface of 0.5% w/v HPMC solution, and then the suspending solutions containing TiO_2 particles were treated ultrasonically for 15−20 min and mechanically vibrated for 2 or 3 min.

The particle sizes of both the powder and nanoparticles suspended in 0.5% w/v HPMC solution following incubation for 12 and 24 h (5 mg/L) were determined using a TecnaiG220 transmission electron microscope (TEM) (FEI Co., USA) operating at 100 kV. In brief, particles were deposited in suspension onto carbon film TEM grids and allowed to dry in air. The mean particle size was determined by measuring >100 randomly sampled individual particles. X-ray-diffraction (XRD) patterns of TiO_2 NPs were obtained at room temperature with a charge-coupled device (CCD) diffractometer (Mercury 3 Versatile CCD Detector; Rigaku Corp., Tokyo, Japan) using Ni-filtered Cu Kα radiation. The surface area of each sample was determined by Brunauer−Emmett−Teller (BET) adsorption measurements on a Micromeritics ASAP 2020M+C instrument (Micromeritics Co., USA). The average aggregate or agglomerate size of the TiO_2 NPs after incubation in 0.5% w/v HPMC solution for 12 and 24 h (5 mg/L) was measured by dynamic light scattering (DLS) using a Zeta PALS + BI-90 Plus (Brookhaven Instruments Corp., USA) at a wavelength of 659 nm. The scattering angle was fixed at 90°. The amount of Ti^{4+} ion leakage from TiO_2 NPs at time 0 and/or after 12, 24, or 48 h of incubation in 0.5% w/v HPMC was measured by inductively coupled plasma-mass spectrometry (ICP-MS, Thermo Elemental X7, Thermo Electron Co., Finland) after the sample was centrifuged at 1719*g* for 10 min and filtered using a 0.001 μm membrane filter.

Animals and Treatment. Female CD-1 (ICR) mice were used in this study; 150 female CD-1 (ICR) mice aged 5 weeks (23 ± 2 g) were purchased from the Animal Center of Soochow University (China).

Table 2. Characteristics of TiO_2 NPs

sample	crystllite size (nm)	phase	surface area (m^2/g)	composition	zeta potential
TiO_2 NPs	5.5	anatase	174.8	Ti, O	7.57,[a] 9.28[b]

[a]Zeta potential after the 12 h incubation in 0.05% w/v HPMC solvent. [b]Zeta potential after the 24 h incubation in 0.05% w/v HPMC solvent.

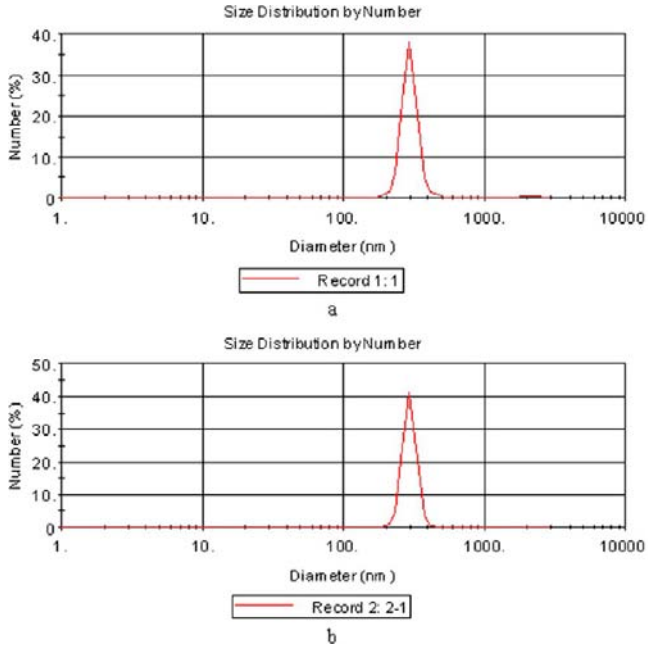

Figure 3. Hydrodynamic diameter distribution of TiO_2 NPs in HPMC solvent using DLS characterization: (a) incubation for 12 h; (b) incubation for 24 h.

dx.doi.org/10.1021/jf3035989 | J. Agric. Food Chem. 2013, 61, 5590−5599

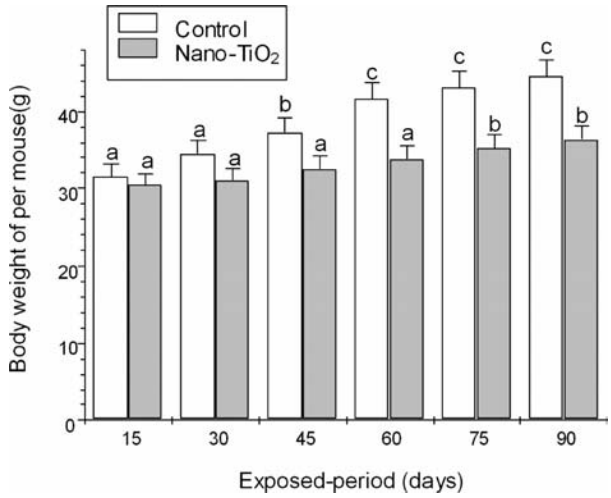

Figure 4. Body weight of mice after intragastric administration of 10 mg/kg BW nano-TiO_2 for different exposure periods. Different letters indicate significant differences between groups ($P < 0.05$). Values represent means ± SEM ($N = 20$).

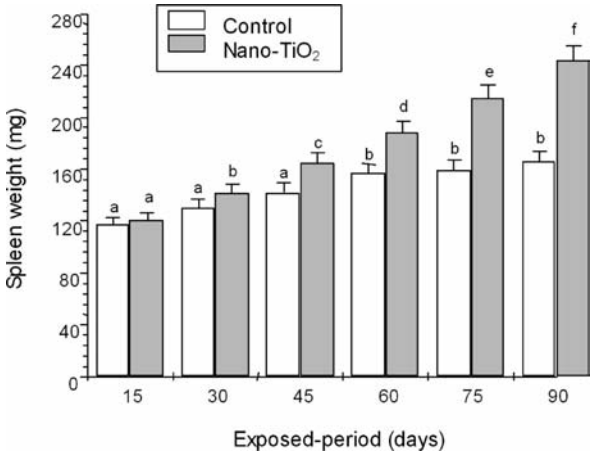

Figure 5. Spleen weight in mice after intragastric administration of 10 mg/kg BW nano-TiO_2 for different exposure periods. Different letters indicate significant differences between groups ($P < 0.05$). Values represent means ± SEM ($N = 20$).

All mice were housed in stainless steel cages in a ventilated animal room. The room temperature of the housing facility was maintained at 24 ± 2 °C with a relative humidity of 60 ± 10% and a 12 h light/dark cycle. Distilled water and sterilized food were available for mice ad libitum. Prior to dosing, the mice were acclimatized to this environment for 5 days.

In the present study, we selected 10 mg/kg BW nano-TiO_2 for intragastric administration each day and used 0.5% HPMC as the suspending agent. Nano-TiO_2 powder was dispersed onto the surface of 0.5% w/v HPMC, and the suspension containing TiO_2 NPs was then treated ultrasonically for 30 min and mechanically vibrated for 5 min. In the experiment, the mice were randomly divided into two groups, a control group (treated with 0.5% w/v HPMC; $N = 20$) and a verum group (10 mg/kg BW nano-TiO_2) divided into six subgroups ($N = 20$). The mice were weighed, and the fresh nano-TiO_2 suspensions were given to the mice by intragastric administration every day for 15, 30, 45, 60, 75, and 90 days, respectively. Any symptoms and mortality were carefully recorded every day during the experimental period. After 15, 30, 45, 60, 75, and 90 days, the mice were weighed and then sacrificed after being anesthetized using ether. The spleens were quickly removed, placed in ice, and then dissected and frozen at −80 °C.

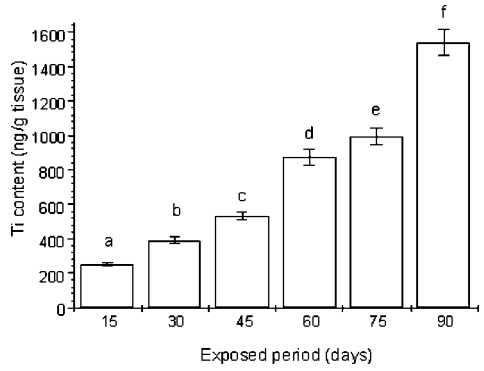

Figure 6. Titanium accumulation in mouse spleen caused by intragastric administration of 10 mg/kg BW nano-TiO_2 for different exposure periods. Different letters indicate significant differences between groups ($P < 0.05$). Values represent means ± SEM ($N = 5$).

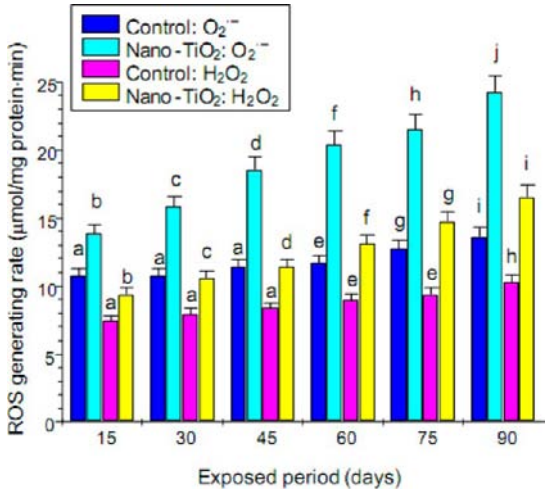

Figure 7. Effect of nano-TiO_2 on ROS production in the spleen following different exposure periods. Different letters indicate significant differences between groups ($P < 0.05$). Values represent means ± SEM ($N = 5$).

Titanium Content Analysis. The spleens were removed from the freezer (−80 °C) and thawed. Approximately 0.2 g of the spleen was weighed, digested, and analyzed for titanium content. ICP-MS (Thermo Elemental X7; Thermo Electron Co., USA) was used to analyze the titanium concentration in the samples.

Histopathological Examination of Spleen. For pathologic studies, all histopathologic examinations were performed using standard laboratory procedures. The spleens were embedded in paraffin blocks, then sliced (5 μm thickness), and placed onto glass slides. After hematoxylin−eosin (HE) staining, the stained sections were evaluated by a histopathologist unaware of the treatments, using an optical microscope (Nikon U-III Multipoint Sensor System, Japan).

Confocal Raman Microscopy of Spleen Sections. Raman analysis was performed using backscattering geometry in a confocal configuration at room temperature in an HR-800 Raman microscopy system equipped with a 632.817 nm HeNe laser (JY Co., France). Laser power and resolution were approximately 20 mW and 0.3 cm^{-1}, respectively, whereas the integration time was adjusted to 1 s. The spleens were embedded in paraffin blocks, then sliced into 5 μm thick sections, and placed onto glass slides. The slides were dewaxed, hydrated, and then scanned under the confocal Raman microscope.

Oxidative Stress Assay. For the ROS assay, $O_2^{\bullet-}$ in the spleen tissues was measured by monitoring the reduction of 3′-{1-[(phenylamino)-carbonyl]-3,4-tetrazolium}bis(4-methoxy-6-nitro)benzenesulfonic acid hydrate (XTT) in the presence of $O_2^{\bullet-}$, as described by Oliveira et al.[33]

dx.doi.org/10.1021/jf3035989 | J. Agric. Food Chem. 2013, 61, 5590−5599

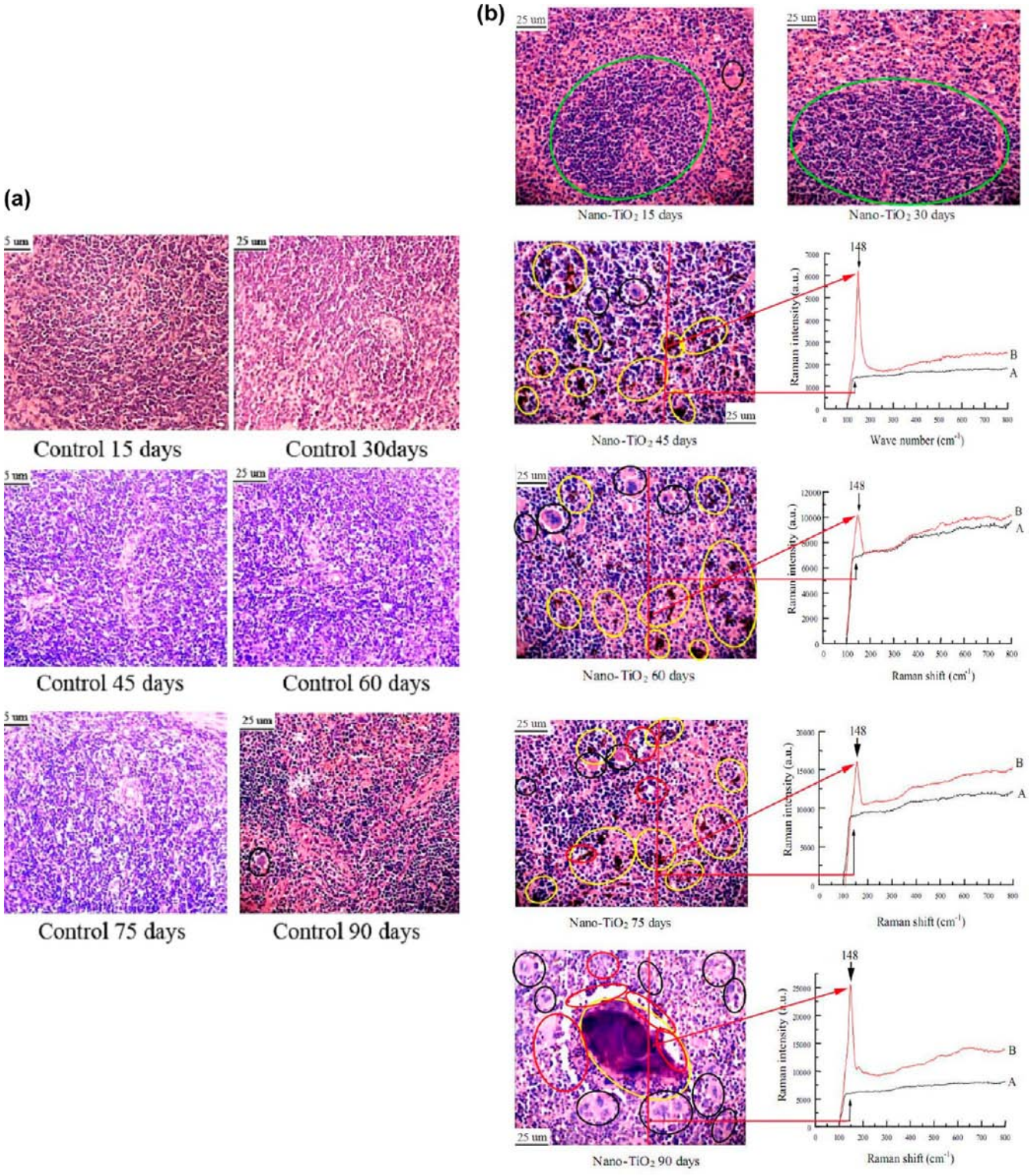

Figure 8. Histopathological changes in the spleen and confocal Raman analysis of the dispersed nano-TiO_2 in the spleen caused by intragastric administration of nano-TiO_2 for different exposure periods: (a) control groups; (b) 10 mg/kg nano-TiO_2 groups. Black circle indicates macrophage infiltration, green circle indicates lymphocyte proliferation, yellow circle indicates nano-TiO_2 aggregation, and red circle indicates fatty degeneration or cell necrosis. Arrow A spot is a representative cell that did not engulf the nano-TiO_2, whereas arrow B spot denotes a representative cell loaded with nano-TiO_2. The right panels show the corresponding Raman spectra identifying the specific peaks at about 148 cm^{-1}.

The detection of H_2O_2 in lung tissues was carried out using the xylenol orange assay.[34]

Assay of Cytokine Expression. The levels of mRNA expression of *COX-2*, *PGE2*, *AP-1*, *CRE*, *Akt*, *PI3-K*, *MAPKs*, *JNK*, *ERK*, *c-Jun*, and *c-Fos* in mouse spleen tissues were determined using real-time quantitative RT polymerase chain reaction (RT-PCR).[35−37] Synthesized cDNA was used for the real-time PCR by employing primers that were designed using Primer Express software according to the software guidelines. The PCR primer sequences are listed in Table 1. To determine COX-2, PGE2, AP-1, CRE, Akt, PI3-K, MAPKs, JNK, ERK,

dx.doi.org/10.1021/jf3035989 | J. Agric. Food Chem. 2013, 61, 5590−5599

c-Jun, and c-Fos levels in mouse spleen tissues, ELISA was performed using commercial kits that were selective for each respective protein (R&D Systems, USA), following the manufacturer's instructions. The absorbance was measured on a microplate reader at 450 nm (Varioskan Flash, Thermo Electron, Finland), and the concentrations of COX-2, PGE2, AP-1, CRE, Akt, PI3-K, MAPKs, JNK, ERK, c-Jun, and c-Fos were calculated from a standard curve for each sample.

Statistical Analysis. All results are expressed as means ± standard error of the mean (SEM). Significant differences were examined by unpaired Student's *t* test using SPSS 19 software (USA). A *P* value of <0.05 was considered to be statistically significant.

RESULTS

TiO_2 NPs Characteristics. XRD measurements show that TiO_2 NPs exhibit the anatase structure (Figure 1), and the average grain size calculated from the broadening of the (101) XRD peak of anatase was roughly 5.5 nm using Scherrer's equation. TEM demonstrated that the average size of the powder particles (Figure 2a) and nanoparticles suspended in HPMC solvent after 12 and 24 h of incubation ranged from 5 to 6 nm, respectively (Figure 2b,c), which was consistent with the XRD results. The value of the sample surface area was generally smaller than that estimated from the particle size, and it would seem that aggregation of the particles may cause such a decrease (Table 2). To investigate the dispersion and stability of the suspensions of TiO_2 NPs, we determined the aggregated size and zeta potential of TiO_2 NPs in HPMC. After 12 and 24 h of incubation, the mean hydrodynamic diameter of TiO_2 NPs in HPMC solvent ranged between 208 and 330 nm (mainly 294 nm), as measured by DLS (Figure 3), which indicated that the majority of TiO_2 NPs were clustered and aggregated in solution. In addition, the zeta potential was 7.57 and 9.28 mV, respectively. The particle characteristics of the TiO_2 NPs used in this study are summarized in Table 2. The leakage of Ti^{4+} ions during 12, 24, and 48 h of incubation of TiO_2 NPs in HPMC solvent after centrifugation was measured by ICP-MS. However, Ti^{4+} contents were not detected in the filtrate, which were lower than the detection limit of 0.074 ng/mL (not listed). Therefore, these results suggested that Ti^{4+} ion leakage from TiO_2 NPs is limited during incubation in HPMC.

Body Weight, Spleen Weight, and Titanium Accumulation. At different experimental time periods, all mice and their spleens were accurately weighed. Figure 4 shows the body weights of the mice. The body weights in the nano-TiO_2-treated groups following 15 and 30 days of exposure were lower than those in the control group; however, these differences were not statistically significant ($P > 0.05$), respectively. In the nano-TiO_2-treated groups following 45, 60, and 90 days of exposure, the body weights were significantly lower ($P < 0.05$ or 0.01) than those in the controls, respectively, suggesting that increased exposure duration to nano-TiO_2 affected the growth of mice. Furthermore, it can be seen from Figure 5 that exposure to nano-TiO_2 caused increases in spleen weight when the exposure period increased ($P < 0.05$ or 0.01). Titanium accumulation in spleen tissue was measured by ICP-MS (Figure 6). Significant titanium accumulation was observed with increased nano-TiO_2 exposure ($P \ll 0.01$); however, in unexposed mice, titanium was not detected. This demonstrated that the accumulation of administered nano-TiO_2 in the spleen may be closely related to body weight, spleen weight, and spleen injury in mice in a time-dependent manner, which was confirmed by further histopathological observation of spleen.

ROS Production. To determine whether nano-TiO_2 stimulated the spleen to produce ROS, we measured the rate of ROS generation in the spleen after treatment with 10 mg/kg BW nano-TiO_2 for various exposure periods. With increased exposure duration, nano-TiO_2 significantly increased ROS production in the spleen (Figure 7).

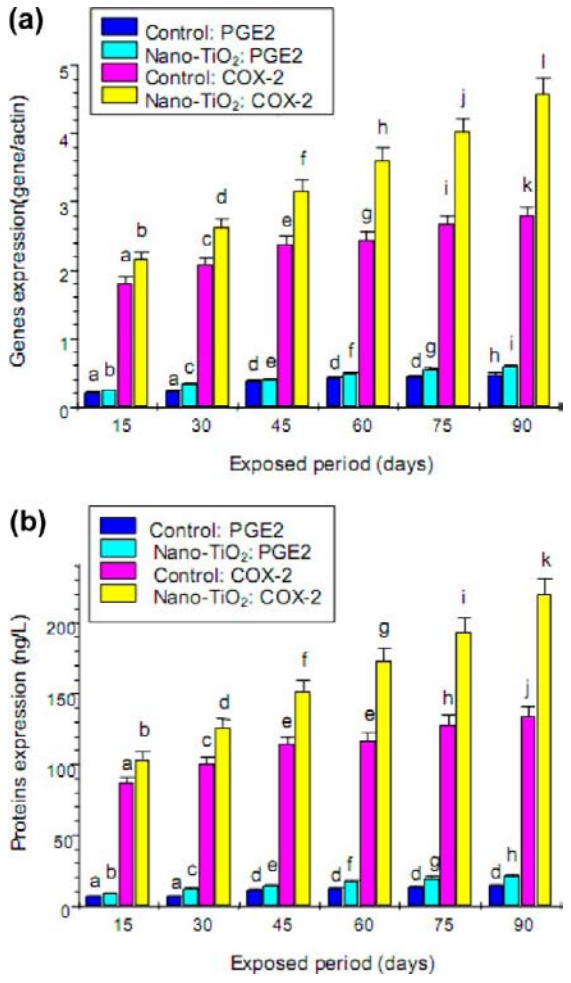

Figure 9. Effects of nano-TiO_2 on PGE2 and COX-2 expression in the spleen following different exposure periods. Different letters indicate significant differences between groups ($P < 0.05$). Values represent means ± SEM ($N = 5$).

Histopathological Evaluation and Raman Analysis of the Dispersed Nano-TiO_2. The histological changes in the spleen are shown in Figure 8. Unexposed spleen did not exhibit any histological changes during the experimental period (Figure 8a); however, with increased exposure duration, the nano-TiO_2-treated groups exhibited severe histological changes, including lymphocyte proliferation, macrophage infiltration, fatty degeneration, and cell necrosis in the spleen (Figure 8b), respectively. In addition, we observed black agglomerates in 10 mg/kg BW nano-TiO_2-exposed female mice (Figure 8b). Furthermore, confocal Raman microscopy showed characteristic nano-TiO_2 peaks (148 cm^{-1}) in the spleens of mice exposed for 45, 60, 75, and 90 days, which further confirmed the presence of nano-TiO_2 in these spleen areas (see spectrum B in the Raman insets in Figure 8b). The results also suggested that nano-TiO_2 was deposited in the spleen in a time-dependent manner and resulted in spleen injury.

Induction of COX-2 Expression. The effects of nano-TiO_2 treatment on PGE2 and COX-2 gene and protein expression were assessed in the spleen. Exposure to nano-TiO_2 from day 15 to day 90 significantly increased the expression of PGE2 ($P < 0.05$),

dx.doi.org/10.1021/jf3035989 | J. Agric. Food Chem. 2013, 61, 5590−5599

one of the major metabolites of COX-2 (Figure 9). To explain the observed PGE2 elevation due to nano-TiO_2, the COX-2 gene and its protein level were measured by RT-PCR and ELISA, respectively. Nano-TiO_2 was found to significantly increase COX-2 expression levels with increased exposure duration ($P < 0.05$) (Figure 9). Therefore, exposure to nano-TiO_2 markedly promoted the expression of both PGE and COX-2 in the spleen.

Expression of AP-1 and CRE of COX-2 Promoter. To investigate the molecular mechanism of nano-TiO_2 action during COX-2 induction, the levels of several transcription factors, including AP-1 and CRE, were analyzed by RT-PCR and ELISA. With increased exposure duration, the expression levels of AP-1 and CRE genes and their proteins in spleen were gradually elevated, and the levels in nano-TiO_2-exposed mice were higher than those in unexposed mice ($P < 0.05$ or 0.01) (Figure 10). In addition, exposure to nano-TiO_2 also increased

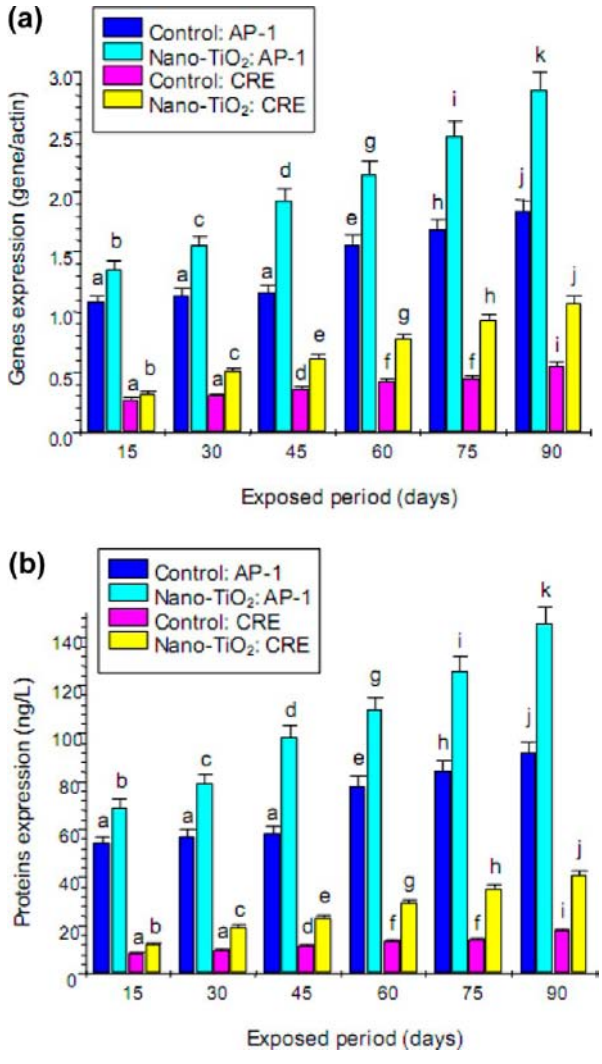

Figure 10. Effects of nano-TiO_2 on protein expression of AP-1 and CRE elements of the COX-2 promoter in spleen following different exposure periods. Letters indicate significant differences between groups ($P < 0.05$). Values represent means ± SE ($N = 5$).

the expression levels of c-Jun and c-Fos genes and proteins of AP-1 promoter in a time-dependent manner in the spleen (Figure 11).

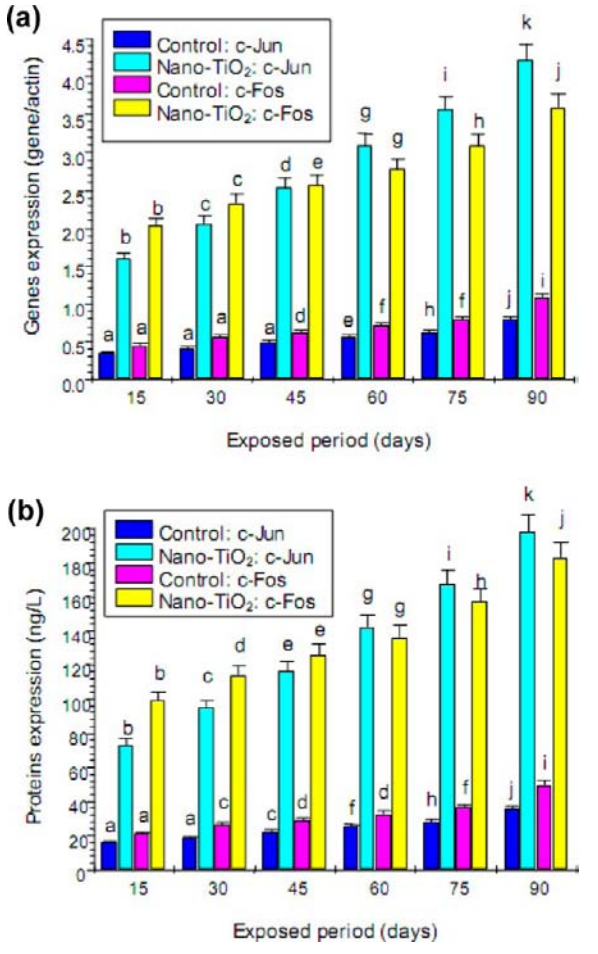

Figure 11. Effects of nano-TiO_2 on protein expression of c-Jun and c-Fos elements of the AP-1 promoter in spleen following different exposure periods. Different letters indicate significant differences between groups ($P < 0.05$). Values represent means ± SEM ($N = 5$).

Induction of MAPKs/PI3-K/Akt Signaling Pathways. MAPKs and PI3-K/Akt are important signaling modulators in COX-2 expression. Therefore, the involvement of MAPKs/PI-3K/Akt signaling pathways in nano-TiO_2-induced COX-2 expression was investigated. It was observed that exposure to nano-TiO_2 significantly elevated the expression levels of Akt, JNKs, MAPKs, PI3-K, and ERK genes and proteins in the spleen, and the expression levels were significantly higher than those in the control group ($P < 0.05$ or 0.01) (Tables 3 and 4). These results showed that nano-TiO_2 markedly up-regulated the expression of COX-2 gene and its protein through the MAPKs/PI-3K/Akt signaling pathways in the spleen.

DISCUSSION

In the present study, multiple exposure to nano-TiO_2 led to increased deposition in mouse spleen (Figures 6 and 8b) and resulted in significant decreases in body weight gain (Figure 4) and gradual increases in spleen weight (Figure 5), ROS accumulation (such as $O_2^{\bullet-}$ and H_2O_2) (Figure 7), and injuries including excessive lymphocyte proliferation, excessive macrophage infiltration, fatty degeneration, and cell necrosis (Figure 8b) in mouse spleen. Our previous study also indicated that 90 days of exposure to 10 mg/kg nano-TiO_2 by gavage resulted in significant splenomegaly, lymphocyte overproliferation, and splenocyte apoptosis in mouse spleen.[10] It is known that excessive lymphocyte

dx.doi.org/10.1021/jf3035989 | J. Agric. Food Chem. 2013, 61, 5590−5599

Table 3. Exposure to TIO_2 NPs Activates MAPKs/PI3-K/Akt Signaling Pathways in Mouse Spleen[a]

gene expression (gene/actin)		exposure term					
		15 days	30 days	45 days	60 days	75 days	90 days
Akt	control	0.51 ± 0.03a	0.60 ± 0.03a	0.76 ± 0.04b	0.88 ± 0.04b	0.97 ± 0.05c	1.09 ± 0.05c
	TiO_2 NPs	0.73 ± 0.04b	0.83 ± 0.04b	1.09 ± 0.05c	1.26 ± 0.06d	1.71 ± 0.09e	2.04 ± 0.10f
JNK2	control	0.22 ± 0.01a	0.27 ± 0.015b	0.35 ± 0.02c	0.37 ± 0.02c	0.52 ± 0.03d	0.56 ± 0.03d
	TiO_2 NPs	0.25 ± 0.01a	0.34 ± 0.02c	0.45 ± 0.02c	0.57 ± 0.03d	0.66 ± 0.03d	0.85 ± 0.04e
MAPK	control	2.26 ± 0.11a	2.51 ± 0.13b	2.83 ± 0.14c	3.25 ± 0.16d	3.71 ± 0.19e	4.20 ± 0.21f
	TiO_2 NPs	2.54 ± 0.13b	2.78 ± 0.14c	3.85 ± 0.19e	5.01 ± 0.25g	6.23 ± 0.31h	7.35 ± 0.37i
PI3-kinase (p38)	control	2.46 ± 0.12a	2.70 ± 0.14b	2.89 ± 0.15c	3.96 ± 0.20d	4.73 ± 0.24e	5.59 ± 0.28f
	TiO_2 NPs	2.73 ± 0.14b	3.80 ± 0.19d	4.69 ± 0.23e	5.75 ± 0.29f	6.40 ± 0.32h	7.27 ± 0.37i
ERK	control	1.29 ± 0.069a	1.42 ± 0.07b	1.57 ± 0.08c	1.69 ± 0.08d	1.82 ± 0.09e	2.34 ± 0.12f
	TiO_2 NPs	1.40 ± 0.07b	1.49 ± 0.07b	1.96 ± 0.10g	2.24 ± 0.11h	2.64 ± 0.13i	2.98 ± 0.15j

[a]Different letters indicate significant differences between groups ($P < 0.05$). Values represent means ± SEM ($N = 5$).

Table 4. Exposure to TiO_2 NPs Activates MAPKs/PI3-K/Akt Signaling Pathways in Mouse Spleen[a]

protein expression (ng/L)		exposure term					
		15 days	30 days	45 days	60 days	75 days	90 days
Akt	control	7.66 ± 0.38a	9.00 ± 0.45b	11.43 ± 0.57c	13.15 ± 0.66d	14.57 ± 0.73e	16.28 ± 0.81f
	TiO_2 NPs	10.95 ± 0.55c	12.48 ± 0.62d	16.32 ± 0.82f	18.97 ± 0.95g	25.63 ± 1.28h	30.57 ± 1.53i
JNK2	control	2.80 ± 0.14a	3.51 ± 0.18b	4.58 ± 0.23c	4.81 ± 0.24c	6.75 ± 0.34d	7.26 ± 0.36e
	TiO_2 NFs	3.55 ± 0.18b	4.81 ± 0.24c	6.36 ± 0.32d	7.92 ± 0.40f	9.25 ± 0.46g	11.93 ± 0.60h
MAPK	control	38.34 ± 1.92a	42.75 ± 2.14b	48.11 ± 2.41c	55.22 ± 2.76d	63.12 ± 3.16e	71.41 ± 3.57f
	TiO_2 NPs	48.22 ± 2.41c	52.81 ± 2.64g	73.12 ± 3.66f	95.24 ± 4.76h	118.30 ± 5.9i	139.71 ± 6.99j
PI3-kinase (p38)	control	47.28 ± 2.36a	51.89 ± 2.59b	55.51 ± 2.7Sc	76.021 ± 3.806d	90.80 ± 4.54e	107.40 ± 5.37f
	TiO_2 NPs	57.33 ± 2.87c	79.84 ± 3.99d	98.58 ± 4.93g	120.7 ± 6.04h	134.32 ± 6.72i	152.60 ± 7.63j
ERK	control	15.43 ± 0.77a	17.08 ± 0.85b	18.78 ± 0.94b	20.25 ± 1.01c	21.78 ± 1.09c	28.02 ± 1.40d
	TiO_2 NPs	21.08 ± 1.05c	26.78 ± 1.34d	35.31 ± 1.77e	40.37 ± 2.02f	47.49 ± 2.37g	53.55 ± 2.68h

[a]Different letters indicate significant differences between groups ($P < 0.05$). Values represent means ± SEM ($N = 5$).

proliferation caused by exposure to nano-TiO_2 is associated with abnormal immune responses, resulting in the release of inflammation-related cytokines, macrophage infiltration, and excessive activation of various cytokines. Although previous studies have confirmed that exposure to different doses of nano-TiO_2 caused splenic damage involving the p38-Nrf-2 signaling pathway,[4] mitochondrial-mediated pathway,[9] and changes in inflammation-related or apoptosis-related cytokines expression,[10] it is essential to determine whether different periods of exposure to nano-TiO_2 affect PGE2 production or MAPK activation and whether transcription factors precede COX-2 expression in damaged mouse spleen. Therefore, this study was designed to explore whether the splenic injury caused by different periods of exposure to nano-TiO_2 was associated with COX-2 expression in mouse spleen.

In the present study, our data suggested that nano-TiO_2 significantly elevated the levels of PGE2, COX-2 genes, and their protein expression in the spleen following increased exposure duration (Figure 9). It is known that PGE2 is the predominant prostaglandin metabolite produced by COX-2, and increased PGE2 levels occur in various tumors.[38] In addition, PGE2 can affect the immune system by influencing cytokine expression.[39] The effects of COX-2-derived PGE2 on excessive lymphocyte proliferation and apoptosis likely contribute to the splenic injury process following exposure to nano-TiO_2 treatment.

To further investigate the MAPKs/PI-3K/Akt signaling pathways of nano-TiO_2 action during COX-2 induction, the expression levels of the AP-1, CRE transcription factors, c-Jun, c-Fos, Akt, PI3-K, MAPK, ERK, and JNK2 were examined. AP-1 is composed of a heterogeneous set of dimeric proteins, including members of the Jun and Fos family.[40] Multiple signaling pathways regulate the expression of AP-1 and CRE. Several inflammatory stimuli have been demonstrated to induce COX-2 gene expression and to activate MAPKs and PI3-K/Akt.[20,28−30] MAPKs, including ERK, p38, and JNK, are important protein kinases that mediate the post-translational modification of AP-1 and CRE proteins.[41,42] Our findings demonstrated that with increased exposure duration, nano-TiO_2 markedly increased the levels of AP-1, CRE, c-Jun, and c-Fos genes and their proteins (Figures 10 and 11), which in turn led to induction of COX-2 expression. Furthermore, nano-TiO_2 was found to markedly promote the expressions of Akt, PI3-K, MAPK, ERK, and JNK2 cytokines in the spleen (Tables 3 and 4),

dx.doi.org/10.1021/jf3035989 | J. Agric. Food Chem. 2013, 61, 5590−5599

suggesting that PI3-K/Akt may be involved in nano-TiO_2-induced AP-1 and CRE expression, and MAPKs may also be associated with the increased COX-2 expression in mice caused by exposure to nano-TiO_2. Therefore, we consider that nano-TiO_2 significantly up-regulated the expression of COX-2 via the MAPKs/PI-3K/Akt signaling pathways in damaged mouse spleen.

In summary, increased exposure duration to nano-TiO_2 applied perorally resulted in splenic damage, which was closely related to increased COX-2 expression. Nano-TiO_2-induced COX-2 expression appears to be mediated predominantly through induction of AP-1 and CRE in the COX-2 promoter. AP-1/CRE induction following exposure to nano-TiO_2 occurs via the MAPKs/PI-3K/Akt signaling pathways in mouse spleen. Due to an increase in surface area per particle weight, nano-TiO_2 has increased functions as a catalyst compared with non-nano TiO_2. Moreover, due to its particle size, nano-TiO_2 is absorbed into the system and can penetrate into tissues and cells more easily than the non-nano form, which may not be absorbed at all. Therefore, the safety of nano-TiO_2 used in the food industry is of concern.

AUTHOR INFORMATION

Corresponding Author

*Phone: 86-0512-61117563. Fax 86-0512-65880103. E-mail: Hongfsh_cn@sina.com.

Author Contributions

[‖]Xuezi Sang, Bing Li, Yuguan Ze, and Jie Hong contributed equally to this work.

Funding

This work was supported by the National Natural Science Foundation of China (Grants 81273036, 30901218, 30972504, and 81172697), a project funded by the Priority Academic Program Development of Jiangsu Higher Education Institutions, the Major State Basic Research Development Program of China (973 Program) (Grant 2006CB705602), a National Important Project on Scientific Research of China (No. 2011CB933404), the National New Ideas Foundation of Student of China (Grant 111028534), and the "Chun-Tsung scholar" Foundation of Soochow University.

Notes

The authors declare no competing financial interest.

REFERENCES

(1) Powell, J. J.; Faria, N.; Thomas, McKay, E.; Pele, L. C. Origin and fate of dietary nanoparticles and microparticles in the gastrointestinal tract. *J. Autoimmun.* **2010**, *34*, 226−233.

(2) Weir, A.; Westerhoff, P.; Fabricius, L.; Hristovski, K.; von Goetz, N. Titanium dioxide nanoparticles in food and personal care products. *Environ. Sci. Technol.* **2012**, *46*, 2242−2250.

(3) Fayaz, A. M.; Balaji, K.; Girilal, M.; Kalaichelvan, P. T.; Venkatesan, R. Mycobased synthesis of silver nanoparticles and their incorporation into sodium alginate films for vegetable and fruit preservation. *J. Agric. Food Chem.* **2009**, *57*, 6246−6252.

(4) Lopez-Moreno, M. L.; De la Rosa, G.; Hernandez-Viezcas, J. A.; Peralta-Videa, J. R.; Gardea-Torresdey, J. L. X-ray absorption spectroscopy (XAS) corroboration of the uptake and storage of CeO_2 nanoparticles and assessment of their differential toxicity in four hdible plant species. *J. Agric. Food Chem.* **2010**, *58*, 3689−3693.

(5) Goutailler, G.; Guillard, C.; Faure, R.; Païssé, O. Degradation pathway of dicyclanil in water in the presence of titanium dioxide. Comparison with photolysis. *J. Agric. Food Chem.* **2002**, *50*, 5115−5120.

(6) Gimeno, O.; Rivas, F. J.; Beltrán, F. J.; Carbajo, M. Photocatalytic ozonation of winery wastewaters. *J. Agric. Food Chem.* **2007**, *55*, 9944−9950.

(7) Chen, J. Y.; Dong, X.; Zhao, J.; Tang, G. P. In vivo acute toxicity of titanium dioxide nanoparticles to mice after intraperitoneal injection. *J. Appl. Toxicol.* **2009**, *29*, 330−337.

(8) Wang, J.; Li, N.; Zheng, L.; Wang, Y.; Duan, Y. M.; Wang, S. S.; Zhao, X. Y.; Cui, Y. L.; Zhou, M.; Cai, J. W.; Gong, S. J.; Wang, H.; Hong, F. S. P38-Nrf-2 signaling pathway of oxidative stress in mice caused by nanoparticulate TiO_2. *Biol. Trace Elem. Res.* **2011**, *140*, 186−197.

(9) Li, N.; Duan, Y. M.; Hong, M. M.; Zheng, L.; Fei, M.; Zhao, X. Y.; Wang, Y.; Cui, Y. L.; Liu, H. T.; Cai, J. W.; Gong, S. J.; Wang, H.; Hong, F. S. Spleen injury and apoptotic pathway in mice caused by titanium dioxide nanoparticules. *Toxicol. Lett.* **2010**, *195*, 161−168.

(10) Sang, X. Z.; Zheng, L.; Sun, Q. Q.; Li, N.; Cui, Y. L.; Hu, R. P.; Gao, G. D.; Cheng, Z.; Cheng, J.; Gui, S. X.; Liu, H. T.; Zhang, Z. L.; Hong, F. S. The chronic spleen injury of mice following long-period exposure to titanium dioxide nanoparticles. *J. Biomed. Mater. Res. A* **2012**, *100A*, 894−902.

(11) Kuwano, T.; Nakao, S.; Yamamoto, H.; Tsuneyoshi, M.; Yamamoto, T.; Kuwano, M.; Ono, M. Cyclooxygenase 2 is a key enzyme for inflammatory cytokine-induced angiogenesis. *FASEB J.* **2004**, *18*, 300−310.

(12) Fukunaga, K.; Kohli, P.; Bonnans, C.; Fredenburgh, L. E.; Levy, B. D. Cyclooxygenase 2 plays a pivotal role in the resolution of acute lung injury. *J. Immunol.* **2005**, *174*, 5033−5039.

(13) Harris, S. G.; Padilla, J.; Koumas, L.; Ray, D.; Phipps, R. P. Prostaglandins as modulators of immunity. *Trends Immunol.* **2002**, *23*, 144−150.

(14) Tilley, S. L.; Coffman, T. M.; Koller, B. H. Mixed messages: modulation of inflammation and immune responses by prostaglandins and thromboxanes. *J. Clin. Invest.* **2001**, *108*, 15−23.

(15) Goetzl, E. J.; An, S.; Smith, W. L. Specificity of expression and effects of eicosanoid mediators in normal physiology and human diseases. *FASEB J.* **1995**, *9*, 1051−1058.

(16) Phipps, R. P.; Stein, S. H.; Roper, R. L. A new view of prostaglandin E regulation of the immune response. *Immunol. Today* **1991**, *12*, 349−352.

(17) Inoue, H.; Nanayama, T.; Hara, S.; Yokoyama, C.; Tanabe, T. The cyclic AMP response element plays an essential role in the expression of the human prostaglandin-endoperoxide synthase 2 gene in differentiated U937 monocytic cells. *FEBS Lett.* **1994**, *350*, 51−54.

(18) Inoue, H.; Yokoyama, C.; Hara, S.; Tone, Y.; Tanabe, T. Transcriptional regulation of human prostaglandin-endoperoxide synthase-2 gene by lipopolysaccharide and phorbol ester in vascular endothelial cells. Involvement of both nuclear factor for interleukin-6 expression site and cAMP response element. *J. Biol. Chem.* **1995**, *270*, 24965−24971.

(19) Kosaka, T.; Miyata, A.; Ihara, H.; Hara, S.; Sugimoto, T.; Takeda, O.; Takahashi, E.; Tanabe, T. Characterization of the human gene (PTGS2) encoding prostaglandin-endoperoxide synthase 2. *Eur. J. Biochem.* **1994**, *221*, 889−897.

(20) Mestre, J. R.; Subbaramaiah, K.; Sacks, P. G.; Schantz, S. P.; Tanabe, T.; Inoue, H.; Dannenberg, A. J. Retinoids suppress phorbol ester-mediated induction of cyclooxygenase-2. *Cancer Res.* **1997**, *57*, 1081−1085.

(21) Subbaramaiah, K.; Cole, P. A.; Dannenberg, A. J. Retinoids and carnosol suppress cyclooxygenase-2 transcription by CREB-binding protein/p300-dependent and -independent mechanisms. *Cancer Res.* **2002**, *62*, 2522−2530.

(22) Xie, W.; Fletcher, B. S.; Andersen, R. D.; Herschman, H. R. v-src induction of the TIS10/PGS2 prostaglandin synthase gene is mediated by an ATF/CRE transcription response element. *Mol. Cell. Biol.* **1994**, *14*, 6531−6539.

(23) Thomas, B.; Berenbaum, F.; Humbert, L.; Bian, H.; Bérézíat, G.; Crofford, L.; Olivier, J. L. Critical role of C/EBPδ and C/EBPβ factors in the stimulation of the cyclooxygenase-2 gene transcription by

interleukin-1β in articular chondrocytes. *Eur. J. Biochem.* **2000**, *267*, 6798−6809.
(24) Wadleigh, D. J.; Reddy, S. T.; Kopp, E.; Ghosh, S.; Herschman, H. R. Transcriptional activation of the cyclooxygenase-2 gene in endotoxin-treated RAW 264.7 macrophages. *J. Biol. Chem.* **2000**, *275*, 6259−6266.
(25) Hsu, T. C.; Young, M. R.; Cmarik, J.; Colburn, N. H. Activator protein 1 (AP-1) and nuclear factor kappa B (NF-κB)-dependent transcriptional events in carcinogenesis. *Free Radical Biol. Med.* **2000**, *28*, 1338−1348.
(26) Guan, Z.; Buckman, S. Y.; Miller, B. W.; Springer, L. D.; Morrison, A. R. Interleukin 1β-induced cyclooxygenase-2 expression requires activation of both c-Jun NH2-periodinal kinase and p38 MAPK signal pathways in rat renal mesangial cells. *J. Biol. Chem.* **1998**, *273*, 28670−28676.
(27) Ridley, S. H.; Dean, J. L.; Sarsfield, S. J.; Brook, M.; Clark, A. R.; Saklatvala, J. A p38MAP kinase inhibitor regulates stability of interleukin-1-induced cyclooxygenase-2 mRNA. *FEBS Lett.* **1998**, *439*, 75−80.
(28) Pommery, N.; Hénichart, J. P. Involvement of PI3K/Akt pathway in prostate cancer − potential strategies for developing targeted therapies. *Mini-Rev. Med. Chem.* **2005**, *5*, 1125−1132.
(29) Whitmarsh, A. J.; Davis, R. J. Transcription factor AP-1 regulation by mitogen-activated protein kinase signal transduction pathways. *J. Mol. Med.* **1996**, *74*, 589−607.
(30) Roymans, D.; Slegers, H. Phosphatidylinositol 3-kinases in tumor progression. *Eur. J. Biochem.* **2001**, *268*, 487−498.
(31) Yang, P.; Lu, C.; Hua, N.; Du, Y. Titanium dioxide nanoparticles co-doped with Fe^{3+} and Eu^{3+} ions for photocatalysis. *Mater. Lett.* **2002**, *57*, 794−801.
(32) Hu, R. P.; Zheng, L.; Zhang, T.; Cui, Y. L.; Gao, G. D.; Cheng, Z.; Chen, J.; Tang, M.; Hong, F. S. Molecular mechanism of hippocampal apoptosis of mice following exposure to titanium dioxide nanoparticles. *J. Hazard Mater.* **2011**, *191*, 32−40.
(33) Oliveira, C. P.; Lopasso, F. P.; Laurindo, F. R.; Leitao, R. M.; Laudanna, A. A. Protection against liver ischemia-reperfusion injury in rats by silymarin or verapamil. *Transplant Proc.* **2001**, *33*, 3010−3014.
(34) Nourooz-Zadeh, J.; Tajaddini-Sarmadi, J.; Wolff, S. P. Measurement of plasma hydroperoxide concentrations by the ferrous oxidation-xylenol orange assay in conjunction with triphenylphosphine. *Anal. Biochem.* **1994**, *220*, 403−409.
(35) Ke, L. D.; Chen, Z. A reliability test of standard-based quantitative PCR: exogenous vs endogenous standards. *Mol. Cell Probe* **2000**, *14* (2), 127−135.
(36) Livak, K. J.; Schmittgen, T. D. Analysis of relative gene expression data using real-time quantitative PCR and the 2(−ΔΔC-(T)) method. *Methods* **2001**, *25*, 402−408.
(37) Liu, W. H.; Saint, D. A. Validation of a quantitative method for real time PCR kinetics. *Biochem Biophys. Res. Commun.* **2002**, *294*, 347−353.
(38) Mohammed, S. I.; Coffman, K.; Glickman, N. W.; Hayek, M. G.; Waters, D. J.; Schlittler, D.; DeNicola, D. B.; Knapp, D. W. Prostaglandin E2 concentrations in naturally occurring canine cancer. *Prostaglandins, Leukotrienes Essent. Fatty Acids* **2001**, *64*, 1−4.
(39) Stolina, M.; Sharma, S.; Zhu, L.; Dubinett, S. M. Lung cancer cyclooxygenase-2 dependent inhibition of dendritic cell maturation and function. *Proc. Am. Assoc. Cancer Res.* **2000**, *41*, 619.
(40) Karin, M.; Liu, Z.; Zandi, E. AP-1 function and regulation. *Curr. Opin. Cell Biol.* **1997**, *9*, 240−246.
(41) Glinghammar, B.; Inoue, H.; Rafter, J. J. Deoxycholic acid causes DNA damage in colonic cells with subsequent induction of caspases, COX-2 promoter activity and the transcription factors NF-κB and AP-1. *Carcinogenesis* **2002**, *23*, 839−845.
(42) Niederberger, E.; Tegeder, I.; Schafer, C.; Seegel, M.; Grosch, S.; Geisslinger, G. Opposite effects of rofecoxib on nuclear factor-κB and activating protein-1 activation. *J. Pharmacol. Exp. Ther.* **2003**, *304*, 1153−1160.